Influence of orbital symmetry on high-order-harmonic generation and quantum tomography

G. N. Gibson[1,2] and J. Biegert[2,3]
[1]*Department of Physics, University of Connecticut, Storrs, Connecticut 06269, USA*
[2]*Institut de Ciencies Fotoniques, Mediterranean Technology Park, 08860 Castelldefels, Barcelona, Spain*
[3]*Institucio Catalana de Recerca i Estudis Avanc Ats, 08010 Barcelona, Spain*
(Received 20 June 2008; published 19 September 2008)

Quantum tomography based on high-order-harmonic generation in molecules is potentially a powerful technique to image electron orbitals. However, many assumptions are needed to reconstruct the spatial orbital structure from the harmonic spectrum. With two-dimensional model calculations, we examine several of these assumptions and find their validity depends strongly on the orbital symmetry and reconstruction axis. In fact, for certain symmetries we cannot find a reconstruction procedure that gives good results. We compare the length and velocity forms of the dipole interaction and find that the form of the dipole strongly affects the quality of the orbital reconstruction. For all of the wave functions studied, the velocity form works as well or better than the length form and may be the best method for quantum tomography. Moreover, in many cases, using the harmonic radiation polarized perpendicular to the molecular axis gives much better results than the parallel polarization. Finally, we examine the minima in the harmonic spectra as a function of angle and find that they cannot always be interpreted as a two-center interference effect.

DOI: 10.1103/PhysRevA.78.033423 PACS number(s): 33.80.Rv, 32.80.Rm, 42.50.Hz

I. INTRODUCTION

Several years ago, the possibility was raised that the harmonic spectrum generated by molecules in strong laser fields could be used to reconstruct the ground-state orbital of the molecule [1]. This so-called quantum tomography (QT) is particularly exciting as the amplitude of the wave function can, in principle, be recovered, not just the probability density. Reconstruction can only occur because the temporal Fourier transform of the time dependent dipole can be related to the spatial Fourier transform of the ground-state wave function, although this requires numerous assumptions. To become a useful and reliable technique, these assumptions need to be tested in a variety of circumstances to determine exactly how accurate the reconstruction can be [2].

While most work on QT has focused on the ground state of molecules, in this paper, we investigate the possibility of QT on excited states, as this presents some advantages in performing QT and opens up some interesting physics: (1) QT requires spatially aligned molecules, which is generally achieved through impulsive alignment [1,3]. Using the measure of alignment from Ref. [3] (which ranges from 0.5 for random molecules to 1.0 for perfect alignment), alignment factors of 0.65 have been achieved for N_2. However, by exciting a state that has a transition dipole moment parallel to the molecular axis, the excited state population will have a pure $\cos^2(\theta)$ distribution and this distribution has a significantly higher alignment factor of 0.75 without a separate alignment pulse. (2) If the excited state dissociates, one can track the electronic orbital as a function of internuclear separation in a pump-probe experiment, allowing the visualization of the orbital as it progresses from the unified atom limit to the separated atom limit. (3) The influence of enhanced ionization [4] and enhanced excitation [5] due to charge resonant states [6] should be observable at intermediate internuclear separations.

While the reconstruction of excited states is similar to ground states, they present some additional challenges: They come in a much greater variety of orbital symmetries than ground states and the excited states lie closer in energy and may couple more strongly to other excited states, compared to the ground state. This latter aspect may further complicate orbital reconstruction of excited states, but we do not explicitly address this here. Since QT relies on the strong field interaction being in the tunneling regime, longer wavelengths are required for excited states with low binding energies. However, new mid-ir short-pulse laser sources are being developed [7] and will be ideally suited to probing excited states. Thus, our main goal for this paper is to investigate the influence of molecular symmetry on the QT reconstruction algorithm as a first step towards understanding QT of excited states. Moreover, we consider several geometries for QT and study how well they work for different symmetries.

In this paper, we present two types of calculations. First, we find two-dimensional (2D) solutions to the time-dependent Schödinger equation for a model double-well potential in a strong laser field and calculate the harmonic spectrum for two initial states, one with σ_g symmetry and one with σ_u symmetry, as a function of angle between the laser polarization and molecular axes. From this, we can compare the harmonic spectrum in the laboratory frame and the molecular frame and investigate the phase shifts in the harmonic spectrum as a function of angle. Second, for QT, the harmonic spectrum must be related to the Fourier transform of the initial wave-function times the dipole operator. While for exact wave functions, the form of the dipole operator should not matter, it does for the approximate wave functions assumed for QT. Thus, we calculate reconstructed wave functions using the length and velocity form of the dipole moment as these can be used for reconstruction. While the acceleration form gives consistently good results, it cannot be used as the ∇V operator is generally not known.

From these calculations we are led to several conclusions. (1) The length and velocity forms give comparable results, although often the velocity form works better, especially for

π_u states. (2) States with π_g symmetry are poorly reconstructed. Similarly, complex σ_g orbitals are hard to reconstruct. (3) A dispersion equation is needed to connect the frequency domain of the high-order-harmonic generation (HHG) spectrum to the spatial domain of the wave function. We find that

$$k_e^2/2 = n\omega_l + \omega_i \tag{1}$$

is an accurate form of the dispersion relationship, where k_e is the spatial frequency in Fourier space, n is the harmonic order, ω_l is the laser frequency, and ω_i is the binding energy of the initial state ($\omega_i > 0$). This matter has been open to some debate [1,2,8]. (4) The origin of the minima in the harmonic spectrum corresponding to ~180° phase shift observed in both numerical and experimental data [9,15], can be seen directly in the Fourier transform of the orbital wave function. While most of the minima in the harmonic spectra can be explained as a two-center interference effect, we find an additional anomalous minimum when using the acceleration form.

II. CALCULATIONS

Our time-dependent calculations are performed on a 2D spatial grid using the split-operator technique to propagate the 1-electron wave function in time [9,10]. 2D calculations are particularly well suited for investigating QT, as one dimension of the wave function is always projected out by the technique. We use a soft-Coulomb potential which avoids the singularities at the nuclei but preserves a full Rydberg series of excited states [11,12]. It also displays a range of wave-function symmetries. We use the length gauge for the interaction term of the Hamiltonian ($e\mathbf{r}\cdot\mathbf{E}$) which has been shown to give identical results for such 2D grid calculations as the velocity gauge ($\mathbf{p}\cdot\mathbf{A}$) [10]. Once we have obtained the total wave function as a function of time during the laser pulse, we compute the amplitude of the radiated harmonics using the acceleration form [13]

$$\mathbf{A}_{\mathrm{acc}}(\omega) = \int dt \langle \Psi(t) | \nabla V | \Psi(t) \rangle e^{i\omega t}, \tag{2}$$

where $\Psi(t)$ is the total time-dependent wave function and V is the potential.

QT requires the acquisition of harmonic spectra of aligned molecules as a function of angle between the molecular axis and the laser polarization, which requires some discussion: The molecular axis is set by the alignment or excitation laser pulse, while the ionized electron is driven along the direction of the laser polarization. However, the axis of the dipole operator in Eq. (2) is determined by the polarization sensitivities of the detector. Ideally, one would like to measure the polarization of the harmonics along an axis parallel to the molecule. In this case, the dipole operator corotates with the molecular waven function and this simplifies the reconstruction. However, this is not always possible. We consider three detector types. (1) The detector is completely insensitive to polarization, in which case the measured harmonic power is simply the sum of the powers in each component. (2) The detector has some sensitivity to polarization. If the difference in sensitivity is great enough, the two polarization components can be decoupled and transformed into the molecular frame. (3) The detector is sensitive to only one polarization. In this case, the harmonics in the molecular frame can be measured directly. In a polarization insensitive detector [(1), above], the harmonics will be dominated by the polarization along the laser axis, and we refer to this as the laboratory frame. Since it is not always possible to measure the harmonics in the molecular frame, we examine the issues in trying to reconstruct the orbital based on data taken in the laboratory frame.

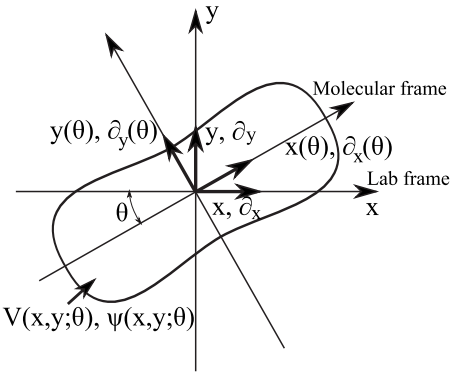

FIG. 1. Various dipole operators and coordinate systems.

Finally, since the harmonic spectrum is supposed to carry the information about the spatial Fourier transform of the wave function, it is far simpler to compute the Fourier transform of the wave functions directly to examine the effects of symmetry on QT. To make the connection between the harmonic spectrum and the spatial wave function, we first write $\Psi(t)$ as the sum of the initial state and a continuum state, which is assumed to be a plane wave [16],

$$\Psi(t) = a\psi_i e^{i\omega_i t} + be^{ik_e x} e^{-i\omega_e t}, \tag{3}$$

where $\omega_e = k_e^2/2$ is the energy of the continuum electron. For weak ionization, $a \approx 1$ and $b \ll 1$. Substituting Eq. (3) into Eq. (2) yields

$$A_{\mathrm{acc}}^{\mathrm{PW}}(\omega,\theta) = \delta(-\omega_i - \omega_e + \omega) \times \int dxdy e^{ik_e x} \partial V(x,y;\theta) \psi_i(x,y;\theta) + \mathrm{c.c.}, \tag{4}$$

where $A_{\mathrm{acc}}^{\mathrm{PW}}(\omega,\theta)$ is the harmonic amplitude in the plane-wave approximation. The laser polarization is along the x axis, the molecule lies in the x-y plane, and the molecular axis makes an angle of θ with respect to the x axis. Thus, the potential and the initial wave function are rotated by an angle θ in the x-y plane, $V(x,y;\theta)$ and $\psi_i(x,y;\theta)$, respectively. Figure 1 shows the various operators and coordinate systems that will be used. In QT, as mentioned above, one axis is always projected out, in this case the z axis.

This form of A_{acc} is very close to the spatial Fourier transform of the radon transform of $\psi_i(x,y)$. The radon transformation is a standard tool in many types of tomography [14].

One problem with Eq. (4) is the presence of the dipole operator ∂V. One can consider Eq. (4) to be the radon transformation of the entire object $\partial V(x,y;\theta)\psi_i(x,y;\theta)$ but we still need to define ∂. There ∂ operator is determined by which component (x or y) of the harmonic polarization $\mathbf{A}$ is measured and in which frame (laboratory or molecular). If the harmonics are measured in the laboratory frame, then $\partial=\partial_x$ corresponds to the harmonics polarization parallel to the laser polarization and $\partial=\partial_y$ corresponds to the perpendicular polarization. It is important to note that ∂_x and ∂_y do not rotate with V and ψ and, so, Eq. (4) does not give a proper radon transformation. However, this does represent the harmonic radiation detected in the laboratory frame and we refer to this as a pseudoradon transformation. Nevertheless, it often leads to a reasonable reconstruction, as we will see. Similarly, if the harmonics are measured in the molecular frame, then $\partial=\partial_x(\theta)$ corresponds to the harmonics polarization parallel to the molecular axis and $\partial=\partial_y(\theta)$ corresponds to those perpendicular to the molecular axis. In this case, $\partial_x(\theta)$ and $\partial_y(\theta)$ do rotate with V and ψ and we have a proper radon transformation. Yet, even in this case, there is still a problem. For example, inverting Eq. (4) for the case of parallel polarization in the molecular frame yields $\partial_x V(x,y)\psi_i(x,y)$. If $\partial_x V(x,y)$ is known, then the ratio of these would finally give $\psi_i(x,y)$. However, $\partial_x V(x,y)$ is generally not known.

This last problem has been addressed by considering the length form of Eqs. (2) and (4),

$$\mathbf{A}_{\mathrm{len}}(\omega)=\omega^2\int dt\langle\Psi(t)|\mathbf{r}|\Psi(t)\rangle e^{i\omega t} \tag{5}$$

and

$$A_{\mathrm{len}}^{\mathrm{PW}}(\omega,\theta)=\delta(-\omega_i-\omega_e+\omega)\omega^2\int dxdye^{ik_e x}r\psi_i(x,y;\theta)+\mathrm{c.c.}, \tag{6}$$

where $r=x$, y, $x(\theta)$, or $y(\theta)$, depending on the measured polarization, as above. In this case, $x\psi_i(x,y)$ is recovered, for example, and the factor x can be divided out [1]. Of course, x goes to zero right down the middle of the wave function. Dividing by x amplifies any noise and errors and leaves an indeterminate line in the reconstruction. This will be true of any of the length dipole operators.

Since the length form of the dipole operator is singular during the reconstruction, we also consider the velocity form

$$\mathbf{A}_{\mathrm{vel}}(\omega)=\omega\int dt\langle\Psi(t)|\boldsymbol{\nabla}|\Psi(t)\rangle e^{i\omega t} \tag{7}$$

and

$$A_{\mathrm{vel}}^{\mathrm{PW}}(\omega,\theta)=\delta(-\omega_i-\omega_e+\omega)\omega\int dxdye^{ik_e x}\partial\psi_i(x,y;\theta)+\mathrm{c.c.} \tag{8}$$

Interestingly, in the velocity form $\partial_x\psi_i(x,y)$, for example, is recovered. This is easily integrated to yield $\psi_i(x,y)$ directly, which is more accurate and immune to noise compared to the length form.

To examine the effects of the form of the dipole operator on the reconstruction, we first calculate $A_{\mathrm{acc}}^{\mathrm{PW}}(\omega,\theta)$, as the acceleration form is presumably the most accurate. Then, a basic assumption of QT is that $A_{\mathrm{len}}^{\mathrm{PW}}(\omega,\theta)=A_{\mathrm{acc}}^{\mathrm{PW}}(\omega,\theta)$ or, alternatively, $A_{\mathrm{vel}}^{\mathrm{PW}}(\omega,\theta)=A_{\mathrm{acc}}^{\mathrm{PW}}(\omega,\theta)$. Using Eqs. (1), (4), (6), and (8) we can write

$$\int dxdye^{ik_e x}r\tilde{\psi}_i(x,y;\theta)=\frac{1}{(k_e^2/2+\omega_i)^2}\int dxdye^{ik_e x}\partial V(x,y;\theta)\psi_i(x,y;\theta) \tag{9}$$

and

$$\int dxdye^{ik_e x}\partial\tilde{\psi}_i(x,y;\theta)=\frac{1}{k_e^2/2+\omega_i}\int dxdye^{ik_e x}\partial V(x,y;\theta)\psi_i(x,y;\theta). \tag{10}$$

where the tilde denotes the recovered wave function.

In the molecular frame, with the harmonics parallel to the molecular axis, we use $\partial=\partial_x(\theta)$ on the right-hand sides of Eqs. (9) and (10). Then, with an inverse Fourier transform and an inverse radon transformation, we obtain $x\tilde{\psi}_i(x,y)$ and $\partial_x\tilde{\psi}_i(x,y)$, respectively. Finally, we can obtain $\tilde{\psi}_i(x,y)$ for each form of the dipole and compare to the original wave function, $\psi_i(x,y)$. We can also consider basing the QT on the harmonics polarized perpendicular to the molecular axis by letting $\partial=\partial_y(\theta)$ on the right-hand sides of Eqs. (9) and (10). This potentially leads to a different $\tilde{\psi}_i(x,y)$ and gives better results for certain symmetries.

In addition to the above reconstruction procedure, we can use the harmonics from the laboratory frame, corresponding to the pseudoradon transformation and simply try to invert the data, anyway. Here we take $\partial=\partial_x$ in Eqs. (9) and (10). In this case, it is not obvious what axis should be used when integrating to remove the ∂ operator in the velocity form, or when dividing to remove the r operator in the length form, as we do not have a proper radon transformation. We tried both $\partial=\partial_x$ and ∂_y in the velocity form and $r=x$ and y in the length form. Interestingly, we found that $\partial=\partial_y$ and $r=y$ worked the best and that is what we present below.

III. RESULTS

A. States with σ_g symmetry

In order to benchmark our calculations, we reproduced the conditions used in Ref. [9]: A 1-electron double-well potential made up of two soft Coulomb potentials with a smoothing factor $\epsilon=0.5$ a.u.^{2} and an internuclear separation of $R=2$ a.u. (a.u. refers to atomic units). The electric field has a pulse shape consisting of 10 optical cycles, which includes a linear turn on and turn off of three cycles, each. We used a wavelength of 800 nm instead of 780 nm as in Ref. [9], but this has only a minor affect on the results. Figure 2(a) shows the initial wave function and Fig. 2(b) shows the logarithmic of the harmonic power spectrum in the labora-

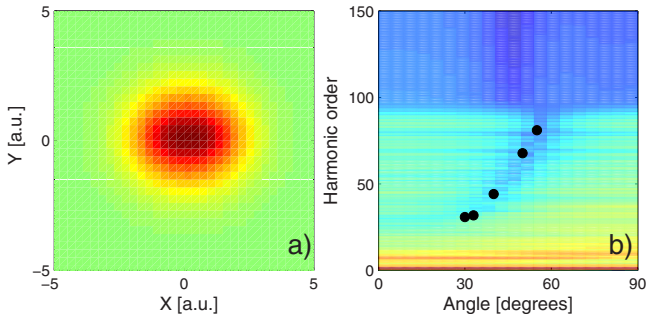

FIG. 2. (Color online) (a) Ground-state wave function. (b) The logarithm of the power spectrum of the harmonics in the laboratory frame from a 2D 1-electron double-well potential, starting in the ground state (σ_g). Black dots show a minimum in the harmonic spectrum as a function of angle from Ref. [9]. The harmonic spectra were smoothed by 1.5 orders to suppress the regular harmonic structure and bring out the envelope of the spectrum.

tory frame as a function of angle between the laser polarization and the molecular axis at an intensity of 5×10^{14} W/cm^2. Overall, the harmonics show a cutoff at around 81, as expected [17] and in agreement with Ref. [9]. However, the more striking feature is the dark valley running through the spectrum. This minimum in harmonic production corresponds to a nodal line and a phase shift of approximately 180° in the harmonic spectrum across the line, as identified in Ref. [9]. Indeed, the black dots show the particular positions of the phase shift of several harmonics as a function of angle given in Ref. [9]. The fact that the dots lie right along the valley indicates excellent agreement between the two calculations.

The reason for the phase shift and corresponding nodal line in the harmonic spectrum has been interpreted as an interference effect, although the explanation has been somewhat convoluted [8,9]. However, if QT is possible, the structure of the harmonic spectrum should correspond to the spatial Fourier transform of the ground-state wave function. Figure 3(a) shows the Fourier transform of the pseudoradon transform of $\partial_x V(x,y;\theta)\psi_i(x,y;\theta)$, or equivalently $A_{\mathrm{acc}}^{\mathrm{PW}}(\omega,\theta)$ from Eq. (4) in k space, in which ∂_x is not rotated.

Immediately apparent is the strong similarity between Figs. 2(b) and 3(a). The same nodal line as a function of angle shows up in the spatial transform of the wave function. However, to make a quantitative comparison, a connection is needed between harmonic order and the k vector of the spatial Fourier transform. In Fig. 3(a), the black dots correspond to those of Fig. 2(b) using the dispersion relationship in Eq. (1). The agreement between the position of the nodal line in the frequency domain and the spatial-frequency domain indicates that Eq. (1) works well.

It has been suggested [9,16] that the nodal lines come from a two-center interference effect. However, the exact interference condition depends on the form of the dipole operator. As is usually done, we assume that the molecular orbital is a linear combination of atomic orbitals (LCAO) centered on each nucleus. We can have a gerade or an ungerade combination of atomic orbitals, $\psi_i^{\pm}=\phi(r-R/2)\pm\phi(r+R/2)$. The dipole matrix element is then

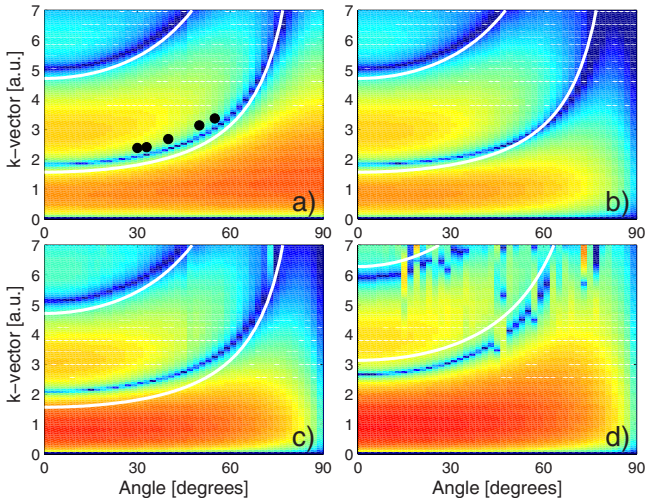

FIG. 3. (Color online) (a) Pseudoradon transformation of $\partial_x V(x,y;\theta)\psi(x,y;\theta)$ for the ground state in Fig. 2(a). Black dots correspond to the dots in Fig. 2(b). (b) Proper radon transformation of $\partial_x(\theta)V(x,y;\theta)\psi(x,y;\theta)$. (c) Proper radon transformation of $\partial_x(\theta)\psi(x,y;\theta)$. (d) Proper radon transformation of $x(\theta)\psi(x,y;\theta)$. Nodal lines predicted from Eqs. (13) and (16) are shown. A logarithmic scale is used. Note, the defects in (d) result from numerical noise.

$$I(k)=\langle e^{ikr}|Q|\psi_i^{\pm}\rangle, \tag{11}$$

where Q is some form of the dipole operator. First, we consider the length form, $Q=x$. If we assume that x is approximately constant over the extent of ϕ, we have

$$x|\psi_i^{\pm}\rangle=\frac{R}{2}[-\phi(r-R/2)\pm\phi(r+R/2)]. \tag{12}$$

The x term leads to a relative sign change between the atomic orbitals. This results in the conditions for destructive interference of

$$\begin{aligned}\mathbf{k}\cdot\mathbf{R}&=2n\pi \quad \text{for } \psi_i^{+}(\text{length})\\ &=(2n+1)\pi \quad \text{for } \psi_i^{-}(\text{length}).\end{aligned} \tag{13}$$

This relative phase shift does not occur for the velocity or acceleration form of the dipole

$$\partial_x|\psi_i\rangle=[\phi'(r-R/2)\pm\phi'(r+R/2)] \tag{14}$$

and

$$\partial_x V|\psi_i\rangle=[V'(r-R/2)\phi(r-R/2)\pm V'(r+R/2)\phi(r+R/2)]. \tag{15}$$

For these cases, the conditions for destructive interference are

$$\begin{aligned}\mathbf{k}\cdot\mathbf{R}&=2n\pi \quad \text{for } \psi_i^{-}(\text{velocity, acceleration})\\ &=(2n+1)\pi \quad \text{for } \psi_i^{+}(\text{velocity, acceleration}).\end{aligned} \tag{16}$$

Of course, this difference only occurs because we are considering imperfect wave functions. Nevertheless, it does highlight the issues associated with the choice of the dipole

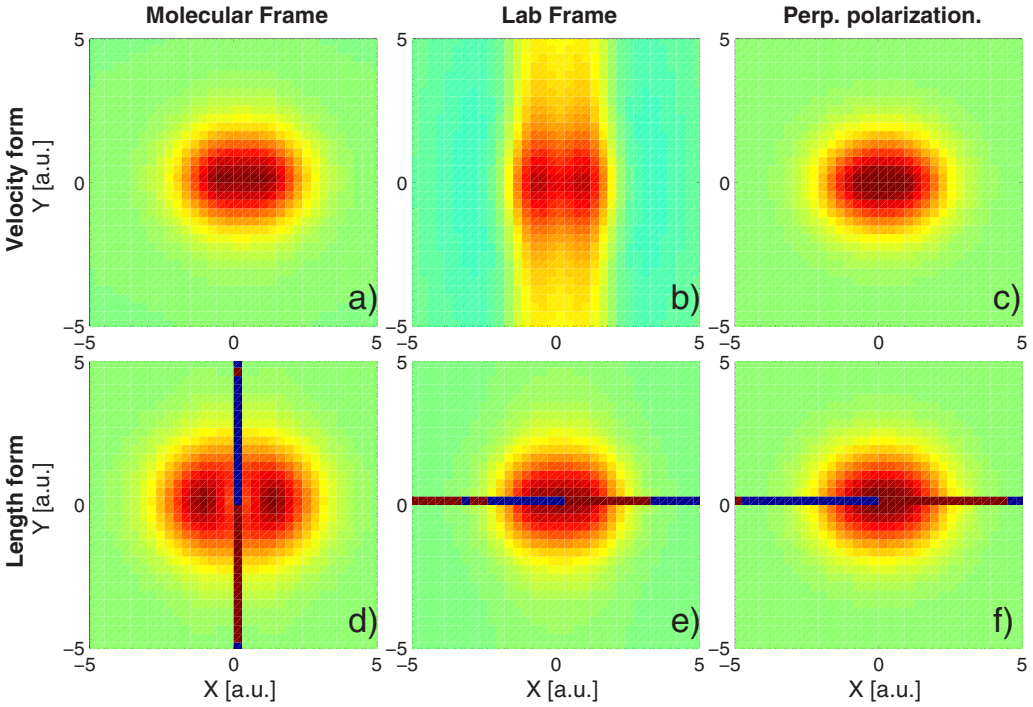

FIG. 4. (Color online) $\tilde{\psi}_i(x,y)$ from the inverse radon transformations of Eqs. (9) and (10) starting with the ground state $\psi_i(x,y)$. (a) Molecular frame data inverted with the velocity form of the dipole. (b) Laboratory frame data (velocity form). (c) Molecular frame data with perpendicular polarization (velocity form). (d) Molecular frame data inverted with the length form of the dipole. (e) Laboratory frame data (length form). (f) Molecular frame data with perpendicular polarization (length form).

operator. Figure 3(a) shows the nodal lines predicted from Eq. (16). The agreement is reasonably good and is only off because of small deviations from the LCAO approximation.

Having established the connection between the harmonic spectrum and the spatial structure of the wave function of the electron, we can address two important issues: First, the difference between the laboratory frame and the molecular frame, and, second, the difference between the length, velocity, and acceleration forms of the dipole interaction. As discussed above, Fig. 3(a) shows the Fourier transform of the pseudoradon transformation of the ground state wave function, which corresponds to the harmonic spectrum in the laboratory frame. Figure 3(b) shows the Fourier transform of the proper radon transformation, which corresponds to the harmonic spectrum in the molecular frame. Superficially, the two transformations look quite similar. In particular, the valley lies in approximately the same place in each plot. The main difference is that in the molecular frame, at 90° the harmonics go to zero, as they should: Harmonics in the molecular frame at 90° would have a polarization perpendicular to the laser polarization, which cannot occur for a symmetric wave function.

To compare the effects of the choice of dipole, Fig. 3(c) shows $A_{\mathrm{vel}}^{\mathrm{PW}}(\omega,\theta)$ from Eq. (8) using a proper radon transformation, and, similarly, Fig. 3(d) shows $A_{\mathrm{len}}^{\mathrm{PW}}(\omega,\theta)$ from Eq. (6). Figures 3(b) and 3(c) are quite similar, as expected, as they share the same interference condition, while Fig. 3(d) clearly shows shifted nodal lines. However, this is in agreement with Eq. (13). Again, it is odd that the interference condition depends on the form of the dipole, but, as mentioned this is only because nonexact wave functions are being considered.

We now examine the effects of the form of the dipole and the choice of laboratory or molecular frame on the wavefunction reconstruction. If we take the inverse radon transformation of the data in the molecular frame using the acceleration form, Fig. 3(b), we should get back the original wave function exactly, after dividing out the $\partial_x V$ term, except that the ∇V operator has many nodal lines which leads to a loss of information upon division. However, as mentioned above, the ∇V operator is not known.

Practical reconstruction can be done using the velocity or length form of the dipole operator. Figure 4(a) shows the result of inverting the data in Fig. 3(b) using the velocity form in the molecular frame [Eq. (10)], to obtain $\tilde{\psi}_i(x,y)$. As can be seen, the results compare very well with the original wave function, Fig. 2(a). This demonstrates that the velocity form of the dipole could lead to a useful reconstruction method, as no knowledge of the potential is required. The results in the laboratory, Fig. 4(b), are not nearly as good, in this case. Finally, Fig. 4(c) shows the results in the molecular frame but using the perpendicular polarization of the harmonics and the results are as good as the parallel polarization.

Previous work on QT has used the length form of the dipole operator for reconstruction, and Figs. 4(d)–4(f) show the same sequence as above, except using the length form of the dipole. Figure 4(d) [using Eq. (9)] has a double peaked structure, in addition to the line running down the middle where x goes to zero. While one might expect results for parallel polarization in the molecular frame to be the best, this is not the case for the length operators. Both the laboratory frame [Fig. 4(e)] and the perpendicular polarization in

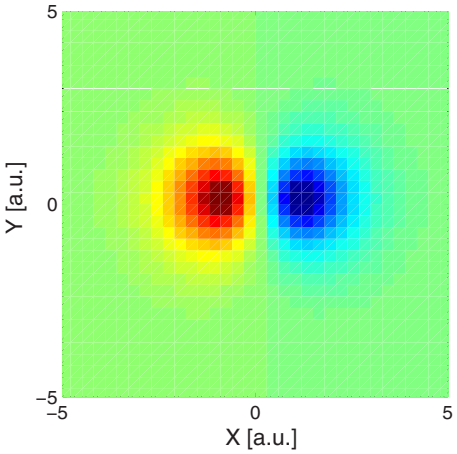

FIG. 5. (Color online) Excited state σ_u wave function.

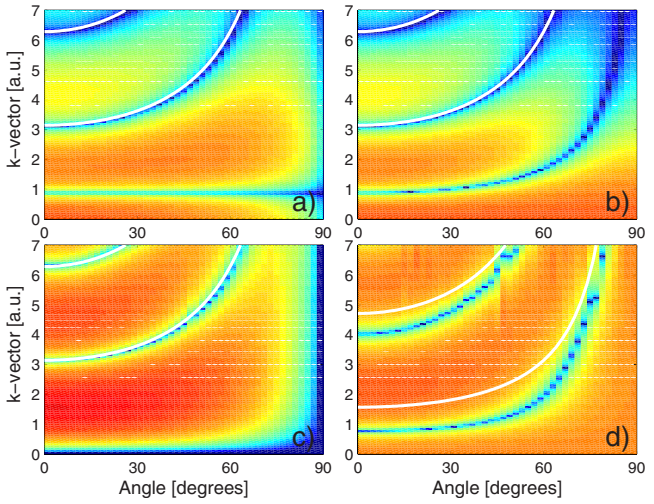

FIG. 6. (Color online) Transforms of σ_u wave function. (a) Pseudoradon transformation of $\partial_x V(x,y;\theta)\psi(x,y;\theta)$. (b) Proper radon transformation of $\partial_x(\theta)V(x,y;\theta)\psi(x,y;\theta)$. (c) Proper radon transformation of $\partial_x(\theta)\psi(x,y;\theta)$. (d) Proper radon transformation of $x(\theta)\psi(x,y;\theta)$. Nodal lines predicted from Eqs. (13) and (16) are shown.

the molecular frame [Fig. 4(f)] give better reconstructions. While this might be a coincidence, this is often the case. Of course, the reconstruction will always have an undetermined line, where, in the latter two cases, the y operator goes to zero.

Before leaving the ground state, we note that we performed the same comparisons with larger internuclear separations of $R=4$ and $R=8$ and the same conclusions hold. This is consistent with the results of Ref. [2] where the authors found that even if the reconstructed wave functions were not perfect, accurate internuclear separations could be determined.

B. States with σ_u symmetry

States with σ_g symmetry are the simplest to reconstruct through QT, while states with lower symmetry present additional problems. To investigate this, we next consider the first excited state of the 2D double-well potential, which has σ_u symmetry. The binding energy of this state is significantly smaller than the ground state. In order to highlight just the changes that result from the different symmetry, we deepen the potential well to achieve the same binding energy as the ground state, above. For this, we need a smoothing parameter $\epsilon=0.0635$ a.u.^{2} and obtain the wave function shown in Fig. 5. Figures 6(a) and 6(b) show the pseudoradon and proper radon transformations of this wave function, respectively, using the acceleration form. Figures 6(c) and 6(d) show the proper radon transformations using the velocity and length forms, respectively, and all graphs show the nodal lines predicted from Eqs. (13) and (16).

For this wave function, the structure of the valleys is quite different between the two frames and between the different choices of the dipole operator. The nodal lines in Figs. 6(a)–6(c), starting at about 3.1 a.u. and 6.3 a.u. at 0°, are predicted quite well by the two-center interference condition. The nodal lines in Fig. 6(d) are close to the predicted lines, but clearly shows the length form is not so good. The most unusual feature in Figs. 6(a) and 6(b) are the additional nodal lines starting at 1 a.u., which are not predicted from a two-center interference effect. Also, its shape changes between the laboratory and molecular frames. Again, this shows that intuition gained with one form of the dipole operator does not necessarily translate to the other forms when imperfect wave functions are considered.

However, an entirely new problem arises: Figures 6(a) and 6(b) predict that at an angle of 90°, the polarization of the harmonics will be completely perpendicular to the laser polarization. Of course, for states of definite parity at 0° or 90°, the harmonics must be polarized along the laser polarization axis, so we need to understand the origin of the discrepancy. Critical to the success of QT is the assumption that the ionized electron returns as a plane wave, Eq. (3). This places a term e^{ikx} in the matrix element giving rise to the harmonic radiation, providing the correct form for a Fourier transform. If the returning electron is not a plane wave, the spatial Fourier transform is lost. The problem comes from the fact that a state with σ_u symmetry rotated by 90° (or alternatively a π_u state at 0°) will have a nodal plane containing the laser polarization axis. The ionized electron will then also have a node along this same plane. This is very much not a plane wave. Indeed, a plane wave traveling along the laser polarization direction and interacting with the above-mentioned orbitals will produce harmonics polarized perpendicular to the laser polarization. The point is that the true ionized electrons are not plane waves and will, as expected, produce harmonics parallel to the laser polarization. Unfortunately, Fig. 6(b), the proper invertible radon transformation of the state in question, will never be recovered. Moreover, calculations using the strong-field approximation [2] will not reproduce this problem, as the electron is still assumed to be a plane wave.

The full quantum evolution of this state is consistent with the above analysis. Figures 7(a) and 7(b) show the harmonic spectrum in the laser and molecular frames, respectively, while Fig. 7(c) shows the molecular frame spectra transformed into k space using the dispersion relationship in Eq.

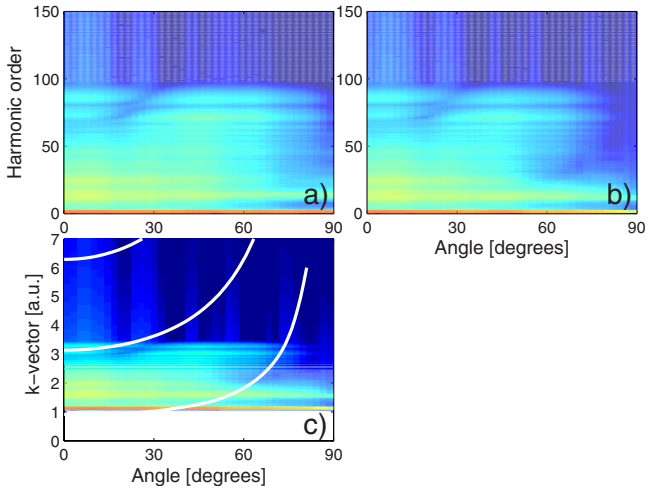

FIG. 7. (Color online) (a) Harmonics as a function of angle in the laboratory frame starting from a state with σ_u symmetry. (b) Harmonics in the molecular frame. (c) Harmonics in the molecular frame transformed into k space. Nodal lines at 3.1 a.u. and 6.3 a.u. are from Eq. (16) while the third line comes from the anomalous nodal line in Fig. 6(b).

(1). Figure 7(c) picks up the nodal line from Fig. 6(b) at roughly the correct k value of 3 a.u., although the harmonic spectrum does not reach high enough to track the nodal line very far. Moreover, the harmonic spectrum in the laboratory frame goes to zero at 90° in both the quantum calculations and the radon transformations, as expected. However, as mentioned above, the laboratory frame is not invertible. Unfortunately, even in the molecular frame, there are problems. The calculated harmonic spectrum in this frame [Fig. 7(b)] has several features that are qualitatively different from the molecular frame radon transformation [Fig. 6(b)]. In the radon transformation, the harmonic spectrum should not go to zero at 90°. As expected from the symmetry the actual harmonic generation does go to zero. Thus, this is a clear example where the harmonic generation is not an adequate probe of the wave function. Moreover, in the radon transformation, there is a second nodal line which carries important information about the wave function. While the harmonics change phase across this line, it is at too large an angle where the actual harmonic spectrum is no longer probing the wave function. Thus, the information in this nodal line is lost. Nevertheless, it does appear that a nodal line is present. The fact that there is evidence for the anomalous nodal line from Fig. 6(b) in Fig. 7(c) suggests that this nodal line is real, despite not being predicted from the two-center interference condition. It also implies that ∇V is the more physical dipole operator.

Finally, we investigate how well σ_u orbitals can be reconstructed. Figure 8 shows reconstructed images of the excited state wave function similar to Fig. 4. On the one hand, for this symmetry, in the molecular frame, the harmonics polarized parallel to the molecular axis do not lead to a useful reconstruction [Figs. 8(a) and 8(d)]. This is due to the problems identified above in the radon transformations in Fig. 6. On the other hand, the perpendicular polarization works extremely well for both forms of the dipole [Figs. 8(c) and 8(f)]. Again, this can be understood by looking at the radon transformations for the perpendicular polarization, shown in Fig. 9. In this case, the molecular frame transforms all look quite similar, leading to similar reconstructions. Again, the

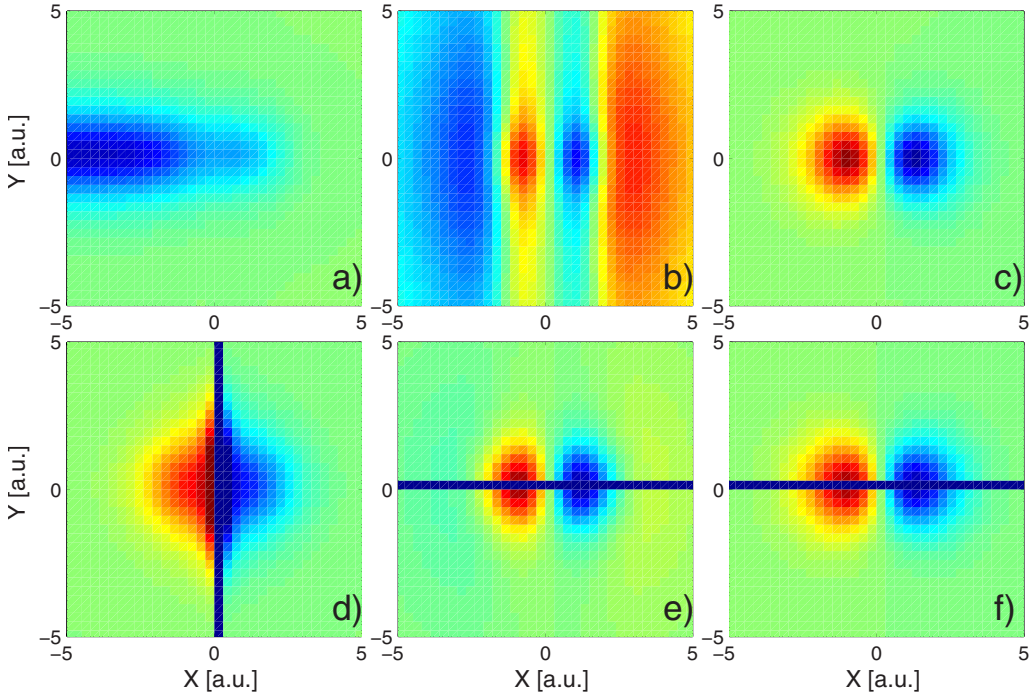

FIG. 8. (Color online) Inverse radon transformations of excited state wave function (R=2). (a) Molecular frame data inverted with the velocity form of the dipole. (b) Laboratory frame data (velocity form). (c) Molecular frame data with perpendicular polarization (velocity form). (d) Molecular frame data inverted with the length form of the dipole. (e) Laboratory frame data (length form). (f) Molecular frame data with perpendicular polarization (length form).

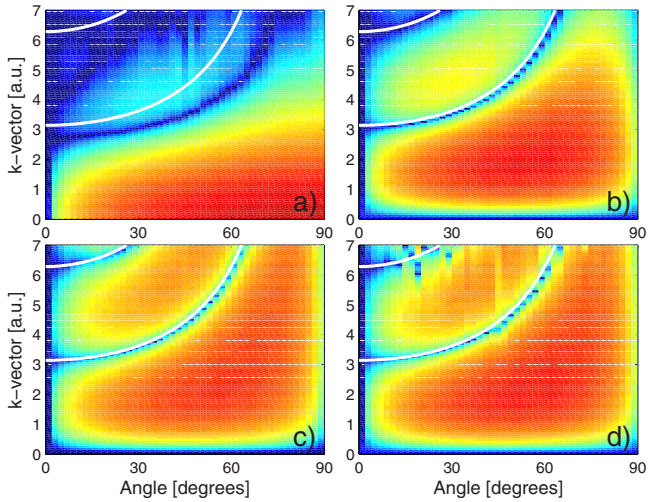

FIG. 9. (Color online) Transforms of σ_u wave function for perpendicular polarization. (a) Pseudoradon transformation of $\partial_y V(x,y;\theta)\psi(x,y;\theta)$. (b) Proper radon transformation of $\partial_y(\theta)V(x,y;\theta)\psi(x,y;\theta)$. (c) Proper radon transformation of $\partial_y(\theta)\psi(x,y;\theta)$. (d) Proper radon transformation of $y(\theta)\psi(x,y;\theta)$. Nodal lines predicted from Eq. (13) are shown. Note that Eq. (16) is not relevant here for the length form in (d), as the dipole operator is y not x. Using y in Eq. (12) does not change the relative sign of the atomic orbitals.

laboratory frame reconstruction with the length form is fairly good.

C. Reconstructing states with other symmetries

In the preceding section, we have found that different reconstruction techniques on wavefunctions with different symmetries give very different results. Thus, in this section, we focus on just the question of reconstruction for some other orbital symmetries, but without full quantum calculations. First, we consider states with π_u symmetry [Fig. 10(a)]. Figure 11 shows the various reconstructed wave functions as in Figs. 4 and 8. This particular symmetry is significant as it is the first one where the length form never gives a reasonable reconstruction, while the velocity form does. In this case, it is the parallel polarization in the molecular frame which works fairly well. Although the shape of the wave function is somewhat distorted, the internuclear separation comes out very well and the π_u character is quite clear.

States with π_g symmetry, not shown, are the most problematic. Neither the length nor the velocity form give reasonable reconstructions using any of methods described above. This represents the most serious failure of this aspect of QT. The length and velocity form of the dipole moment simply do not capture critical elements of the information encoded by the acceleration form.

QT has already been criticized in Ref. [2] in terms of giving quantitative results, but they did find that they could capture the symmetry of the oxygen ground state, which is π_g. This would appear to be in conflict with our inability to reconstruct the π_g orbital. However, it is important to note that in Ref. [2], they used the length form for both calculating the harmonic spectrum [essentially using Eq. (6)] and reconstructing the wave function. They were addressing the question of the limited range of k values probed by the harmonic spectrum and its effect on reconstruction. We are asking whether reconstruction is possible, even with a complete range of k values. In our reconstructed images, if the same form of the dipole is used for generation and reconstruction, the results are very good. What we are attempting to do here is assess the problems induced in using the length and velocity forms of the dipole for reconstruction, while using the acceleration form to generate the harmonic spectrum. Under these conditions, the π_g state cannot be reconstructed.

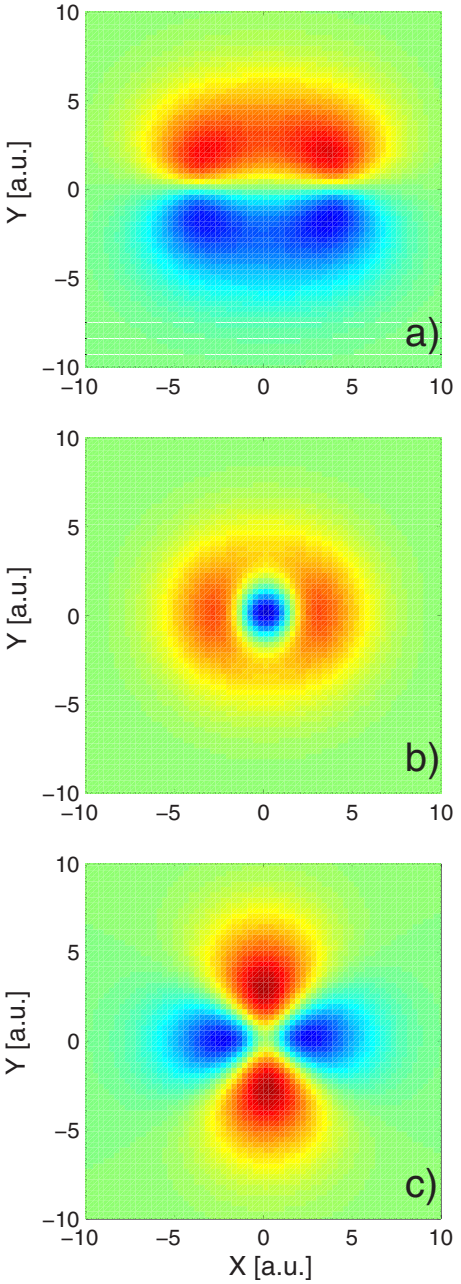

FIG. 10. (Color online) Wave functions of highly excited states. (a) π_u state ($R=8$). (b) σ_g state with hidden structure ($R=2$). (c) σ_g state with side lobes ($R=2$).

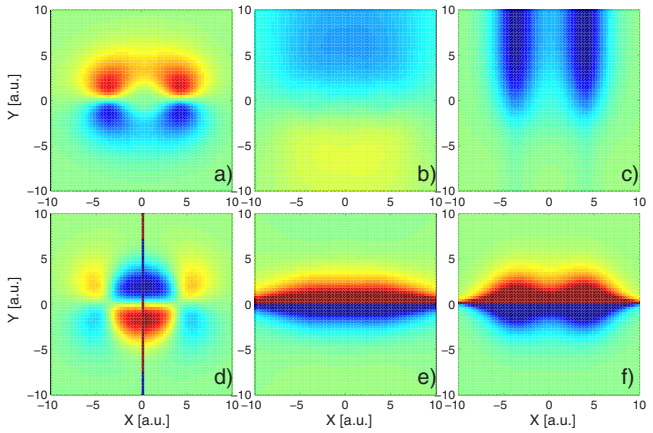

FIG. 11. (Color online) Inverse radon transformations of excited state wave function π_u (R=8). (a) Molecular frame data inverted with the velocity form of the dipole. (b) Laboratory frame data (velocity form). (c) Molecular frame data with perpendicular polarization (velocity form). (d) Molecular frame data inverted with the length form of the dipole. (e) Laboratory frame data (length form). (f) Molecular frame data with perpendicular polarization (length form).

Finally, we have looked at other types of σ_g states, as shown in Figs. 10(b) and 10(c). Generally, the added details of Fig. 10(b) inset structures, known as phantoms in tomography and Fig. 10(c) side lobes are difficult to reconstruct. Figure 12 shows the results of trying to reconstruct Fig. 10(b). In this case, a small negative piece of the wave function is surrounded by a large positive donut. As can be seen in Fig. 12, the central negative piece is hard to recover.

IV. CONCLUSIONS

Clearly, the harmonic spectrum produced by molecules in strong laser fields is intimately connected with the spatial structure of the electronic wave function from which the harmonics are produced, and, thus, the goal of QT is to extract the spatial information from the harmonic spectrum. It has already been shown that this is perhaps asking for too much [2], even within the context of the strong-field approximation. In this paper, we have examined our ability to reconstruct wave functions of various different symmetries. We considered, for the first time, using the velocity form of the dipole operator for wave-function reconstruction. We find that it works as well as the length form in all cases, and, in fact, can reconstruct states with π_u symmetry that the length form cannot. Moreover, it is cleaner, as it never generates indeterminate lines in the reconstruction. We also compared several different reconstruction geometries and found that often the harmonics polarized perpendicular to the molecular axis are better for reconstructing σ orbitals, while the harmonics polarized parallel to the molecular axis are better for π_u orbitals. It turns out that π_g orbitals are very hard to reconstruct. Moreover, details of excited state σ_g orbitals are difficult to recover. Finally, we find that the minima in the harmonic spectra cannot always be described as a two-center interference effect. In summary, by using different dipole operators and reconstruction geometries, we have been able to extend the range of QT to several different orbital symmetries, compared to standard reconstruction techniques, although significant problems still exist for some symmetries.

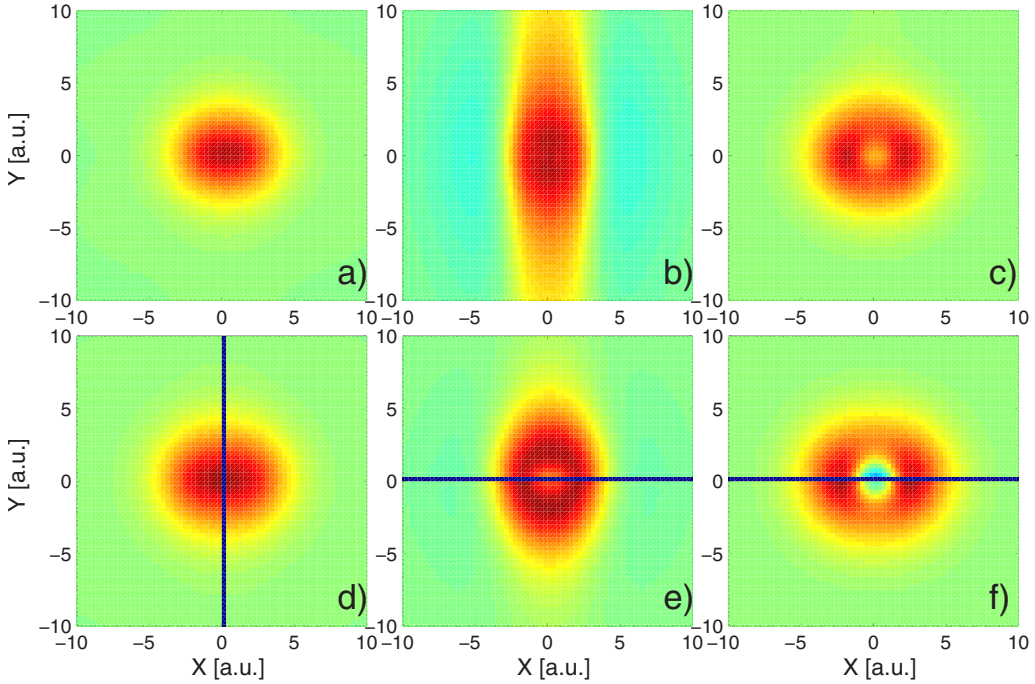

FIG. 12. (Color online) Inverse radon transformations $\tilde{\psi}_i(x,y)$ of Fig. 10(b). (a) Molecular frame data inverted with the velocity form of the dipole. (b) Laboratory frame data (velocity form). (c) Molecular frame data with perpendicular polarization (velocity form). (d) Molecular frame data inverted with the length form of the dipole. (e) Laboratory frame data (length form). (f) Molecular frame data with perpendicular polarization (length form).

ACKNOWLEDGMENTS

This research was carried out with the financial support of the Spanish Ministry of Sciences through Grants No. SAB 2006-0198 and No. CSD2007-00013—Consolider SAUUL. G.N.G. also acknowledges support from the NSF under Grant No. PHYS-0653029. Finally, the authors appreciate useful discussions with Maciej Lewenstein.

[1] J. Itatani, J. Levesque, D. Zeidler, H. Niikura, H. Pépin, J. C. Kieffer, P. B. Corkum, and D. M. Villeneuve, Nature (London) **432**, 867 (2004).
[2] Van-Hoang Le, Anh-Thu Le, Rui-Hua Xie, and C. D. Lin, Phys. Rev. A **76**, 013414 (2007).
[3] P. W. Dooley, I. V. Litvinyuk, K. F. Lee, D. M. Rayner, M. Spanner, D. M. Villeneuve, and P. B. Corkum, Phys. Rev. A **68**, 023406 (2003).
[4] E. Constant, H. Stapelfeldt, and P. B. Corkum, Phys. Rev. Lett. **76**, 4140 (1996).
[5] G. N. Gibson, R. N. Coffee, and L. Fang, Phys. Rev. A **73**, 023418 (2006).
[6] T. Zuo and A. D. Bandrauk, Phys. Rev. A **52**, R2511 (1995).
[7] T. O. Clatterbuck, C. Lyng, P. Colosimo, J. D. D. Martin, B. Sheehy, L. F. Dimauro, P. Agostini, and K. C. Kulander, J. Mod. Opt. **50**, 441 (2003).
[8] X. Zhou, R. Lock, W. Li, N. Wagner, M. M. Murnane, and H. C. Kapteyn, Phys. Rev. Lett. **100**, 073902 (2008).
[9] M. Lein, N. Hay, R. Velotta, J. P. Marangos, and P. L. Knight, Phys. Rev. Lett. **88**, 183903 (2002).
[10] G. N. Gibson, Phys. Rev. A **67**, 043401 (2003).
[11] W.-C. Liu, J. H. Eberly, S. L. Haan, and R. Grobe, Phys. Rev. Lett. **83**, 520 (1999).
[12] I. Kawata, H. Kono, Y. Fujimura, and A. D. Bandrauk, Phys. Rev. A **62**, 031401(R) (2000).
[13] The full acceleration form is $\nabla V + eE$, although the latter term strictly gives the spectrum of the driving field and does not contribute to the high harmonics [9].
[14] http://en.wikipedia.org/wiki/Radon_transformation
[15] W. Boutu, S. Haessler, H. Merdji, P. Breger, G. Waters, M. Stankiewicz, L. J. Frasinski, R. Taieb, J. Caillat, A. Maquet, P. Monchicourt, B. Carre, and P. Salieres, Nat. Phys. **4**, 545 (2008).
[16] G. L. Kamta and A. D. Bandrauk, Phys. Rev. A **71**, 053407 (2005).
[17] P. B. Corkum, Phys. Rev. Lett. **71**, 1994 (1993).